Stability, local structure and electronic properties of borane radicals on the Si(100) 2x1:H surface

A first-principles study

Fang, C.M.; Mohammadi, V.; Nihtianov, S.; Sluiter, M.H.F.

DOI
10.1016/j.commatsci.2017.08.036

Publication date
2017

Document Version
Final published version

Published in
Computational Materials Science

Citation (APA)
Fang, C. M., Mohammadi, V., Nihtianov, S., & Sluiter, M. H. F. (2017). Stability, local structure and electronic properties of borane radicals on the Si(100) 2x1:H surface: A first-principles study. *Computational Materials Science*, *140*(Supplement C), 253 - 260. https://doi.org/10.1016/j.commatsci.2017.08.036

Link to formal publication Computational Materials Science (Elsevier): https://doi.org/10.1016/j.commatsci.2017.08.036

Stability, Local Structure and Electronic Properties of Borane Radicals on the Si(100) 2×1:H Surface: A First-Principles Study

C. M. Fang[1,2,3], V. Mohammadi[2], S. Nihtianov[2] and M. H. F. Sluiter[3]

[1]BCAST, Brunel University London, Waterside House, Cowley Business Park, Uxbridge, Middlesex, UB8 2AD, United Kingdom.

[2]Electronic Instrumentation Lab., Faculty of Electrical Engineering, Mathematics and Computer Science, TU Delft; Mekelweg 4, 2628CD Delft, The Netherlands.

[3]Dept. of Materials Science and Engineering, TU Delft, Mekelweg 2, 2628CD Delft, The Netherlands.

Corresponding authors:

Changming Fang and Marcel Sluiter:

e-mails: Changming.Fang@brunel.ac.uk and M.H.F.Sluiter@tudelft.nl

Abstract

Deposition of a thin B layer via decomposition of B_2H_6 on Si (PureB process) produces B-Si junctions which exhibit unique electronic and optical properties. Here we present the results of our systematic first-principles study of BH_n (n=0 to 3) radicals on Si(100)2×1:H surfaces, the *initial* stage of the PureB process. The calculations reveal an unexpectedly high stability of BH_2 and BH_3 radicals on the surface and a plausible atomic exchange mechanism of surface Si atoms with B atoms from absorbed BH_n radicals. The calculations show strong local structural relaxation and reconstructions, as well as strong chemical bonding between the surface Si and the BH_n radicals. Electronic structure calculations show various defect states in the energy gap of Si due to the BH_n absorption. These results shed light on the *initial* stages of the complicated PureB process and also rationalize the unusual electronic, optical and electrical properties of the deposited Si surfaces.

Key words: Borane deposition; H passivated Si(001) surface; PureB process; Ab initio calculations.

Graphical abstract

The current *ab initio* DFT calculations reveal high stability of BH_2 and BH_3 radicals on the H passivated Si(001) surface and exchange of surface Si with B in the radicals. Furthermore, electronic band structures reveal the formation of various defect states in the Si band gap.

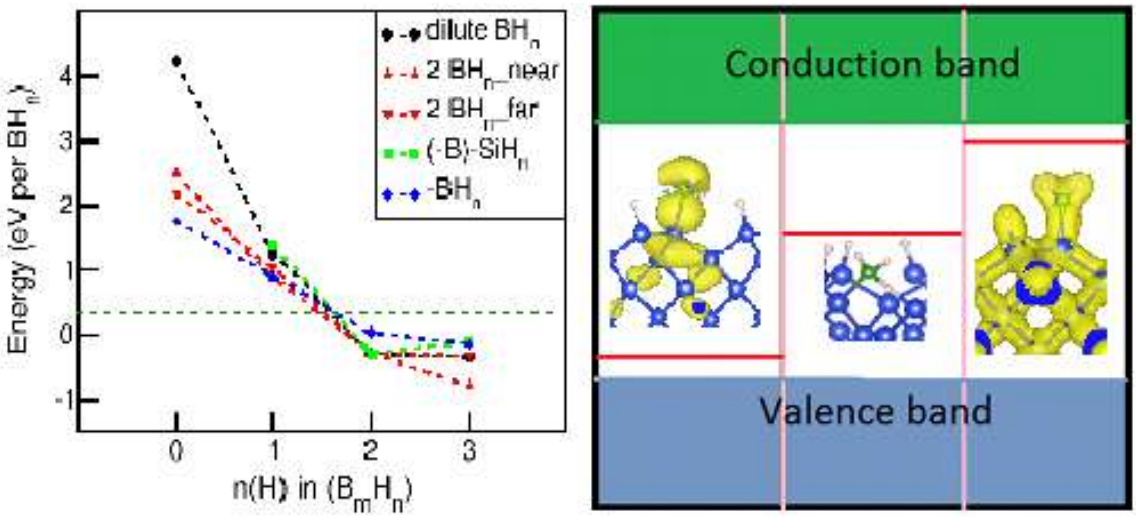

Highlights

1) Structural optimizations show that strong local structural relaxation occurs for dilute depositions of borane radicals on H passivated Si surfaces. Structural reconstructions occur for high concentration borane depositions.

2) There is strong bonding of BH_2 and BH_3 radicals on the Si(001) 2×1:H surface.

3) The total energy calculations reveal possible exchange of surface Si atoms with B in the borane radicals.

4) Electronic band-structure calculations show various defect states formed in the Si bandgap.

5) Thermodynamic analysis shows formation of B and BH radicals on the Si surfaces under low H partial pressure.

I. Introduction

Our interest in this topic stems from both scientific curiosity and the industrial application potential. In the last decade the manufacture of the best performing silicon-based detectors for low-penetration depth radiation has relied on the so-called PureB process. This process involves depositing nano-scale layers of pure boron on Si surfaces by means of chemical vapor deposition (CVD) through diborane (B_2H_6) decomposition [1-7]. Experimental measurements have shown that PureB products have unique electrical and optical properties [2-7]. Interestingly, experiments have also shown that partial coverage (as low as 20 %) of BH_n radicals on Si surfaces modifies the electronic properties of the substrates [4-6]. This suggests the intriguing possibility of controlling the physical properties through the thickness or coverage of the boron layer. It also underlines the crucial importance of utilizing information about the BH_n deposition on Si surfaces at the *initial* stage to fabricate new Si-B devices for applications, such as photodiodes [1,2,7]. Moreover, the BH_n (n=0 to 3) radicals may contain unpaired electrons, that offers potentially new electronic and spintronic properties.

Up to now many experimental efforts have been made to understand the chemical reactions related to the PureB process and the reaction products [1-16]. There were early works on the structure of diborane [8] and its decomposition [9-12]. Later on, various techniques were employed to study the deposition of boron from diborane [13-16]. Habuka *et al.* observed the instability of B_2H_6 gas (molecules) on epitaxial Si films [16]. However, it is difficult to obtain reliable information about B/borane clusters/radicals on Si surfaces due to the complex reaction paths and variable conditions during preparation conditions. In this aspect, theoretical approaches, especially parameter-free first-principles methods are helpful. First-principles approaches have been used successfully to study clean Si surfaces, such as Si(111) reconstructed

$\sqrt{7}a_0 \times \sqrt{7}a_0$ clean surfaces and Si(100) reconstructed $2a_0 \times 1a_0$ surfaces (a_0 is the lattice parameter of bulk Si) [17-19], H-terminated Si surfaces [19], and B in Si [20-22] as well as B on Si surfaces [22-25]. Recently, Shayeganfar and Rochefort investigated electronic properties of a boron-doped Si(111) surfaces by self-assembling trimeric acid [24]. Using first-principles approaches, Hu and co-workers studied gas-reactions between SiH_4 and B_2H_6 and revealed the formation of SiH_4-BH_3-BH_3 as an intermediate product [26]. However, currently there is still a lack of knowledge about boron/borane radicals/clusters on Si surfaces, which play a crucial role in the PureB preparation process at the *initial* stage. Here we present our first-principles study of the BH_n (n=0 to 3) radicals on H-terminated reconstructed Si(001) 2×1 surfaces which have high stability at elevated temperature [19]. Furthermore the silicon wafers with the Si(001) 2×1 surface have been employed in our PureB experiments and related applications [2-7]. The study includes energetics, local structures, chemical bonding and charges at the related atomic sites, as well as electronic properties. This information is necessary to gain insight into PureB-related process, the electronic properties of the products, and further development of applications [1,2,7,25].

II. Computational details

IIa. Reactions and formation energy/enthalpy on Si(001) 2×1:H surfaces: The experiments show that on Si surfaces at elevated temperature, the diborane molecules decompose into two boron tri-hydride molecules as [1-6,12-15]:

$$B_2H_6 \leftrightarrow 2\ BH_3 \qquad (1)$$

This reaction is reversible under the deposition conditions. The reactions of deposition of possible BH_n radicals on the Si surfaces can be described as follows:

$(-)Si\text{-}H + BH_3 \leftrightarrow (-)Si\text{-}B + 2\ H_2 + \Delta H_0$ or/and

$(-)Si\text{-}H + BH_3 \leftrightarrow (-)Si\text{-}BH + 3/2\ H_2 + \Delta H_1$ or/and

$(-)Si\text{-}H + BH_3 \leftrightarrow (-)Si\text{-}BH_2 + H_2 + \Delta H_2$ or/and

$(-)Si\text{-}H + BH_3 \leftrightarrow (-)Si\text{-}BH_3 + \frac{1}{2}\ H_2 + \Delta H_3$

The above reactions can be summarized as:

$$(-)Si\text{-}H + BH_3 \leftrightarrow (-)Si\text{-}BH_n + (2 - n/2)H_2 + \Delta H_n \quad (2)$$

The related formation enthalpy $-\Delta H_n$ can be presented as:

$$-\Delta H_n = \{H[(-)Si\text{-}BH_n] + (4\text{-}n)/2\ H[H_2] - \{H[(-)Si\text{-}H] + H(BH_3)\} \quad (3)$$

Here, $H\{(-)Si\text{-}H\}$, $H[(-)Si\text{-}BH_n]$, $H(BH_3)$ and $H(H_2)$ represent the enthalpies of the H-passivated Si surface, the surface with BH_n absorption $[(-)Si\text{-}BH_n]$ with respect to isolated BH_3 molecule and H_2 molecules. At temperature $T = 0$ K, and pressure $P = 0$ Pa, the enthalpies of the silicon surface systems as well as other terms, such as that of the H_2 molecules, are equal to the corresponding total energies which can be obtained from our first-principles calculations. We neglect the contribution from zero-point vibration. A negative value of the formation enthalpy indicates that reaction is exothermic.

IIb. Si(001) 2×1 surfaces: Bulk Si has a diamond-type structure in which each Si has a tetragonal coordination [27]. A cleavage perpendicular to the {100} axis produces two Si(100) surfaces at which each surface Si atom has only two nearest neighbors from the subsurface layer.

This pristine Si(100) surface is unstable. It is reconstructed into a 2×1 domain in which each surface Si has three neighbors [19]. Under a hydrogen atmosphere, H-passivation restores Si to tetragonal coordination with three Si neighbors below and one H on top (Figure 1a) [19]. The H-passivated Si(001) surface with 2×1 reconstruction (Si(001) 2×1:H) is highly stable at elevated temperature [1-6;17-19]. The H bonding to the Si(100) surface is strong and our calculations show that formation of one dangling Si bond at the surface costs about 1.6 eV. The experiments show that under pure H_2 atmosphere condition, no B layer is formed on the Si surfaces [2-7]. That indicates that creation of Si dangling bonds at the surface requires a H deficient condition. This is realized by employing atmospheres of various H_2/N_2 ratios with low H partial pressure. Furthermore, the PureB processes occurs only at reasonably high temperature (700 to 1000 K) [2-7].

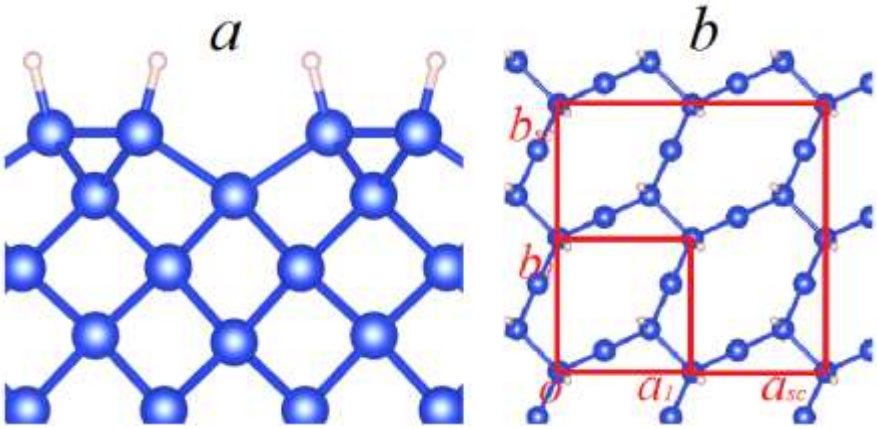

Figure 1. Schematic structures of one H-passivated Si(100) 2×1 surface along (100) orientation (a) and along (001) orientation (b). The red lines in 1b indicate the *a*- and *b*-axes of a reconstructed Si(100) 2×1 primitive unit cell with the a_1- and b_1-axes, and a $2a_1 \times 2a_1$ supercell. The small white (large blue) spheres represent H (Si).

In our calculations periodic boundary conditions (PBCs) were employed. To simulate BH_n (n=0 to 3) radicals on the surface, as well as interaction between the deposited clusters on the surface,

we also employed a $2a_1 \times 2a_1$ supercell for the H-passivated Si(100) 2×1 surface (Figure 1b) (a_1 is the lattice parameter of a conventional cell). This supercell has an edge of about 10.9 Å and it contains 8 surface Si atoms or 4 Si-Si pairs. Such a large supercell can provide information about dilute BH_n deposition on the surface.

In the supercell there are eight Si atoms/ions at each atomic layer (AL). The slab contains 10 Si AL. Therefore, the supercell used in the present study contains 80 Si atoms. Between the interfaces, there is vacuum of (>12 Å) to minimize the interaction between the surfaces as well as the interaction of atoms/molecules absorbed on one surface with another surface. Simulations with two BH_n clusters were performed on the $2a_1 \times 2a_1$ supercell of the Si(001) 2×1 surface. Interaction between the two BH_n clusters on the surface is realized by placing them on two bridging Si atoms nearby or on two separated surface Si atoms. In order to simulate isolated BH_3 and H_2 molecules as references a large cube with an axis length of about 20 Å was employed. We analyzed the charges at, and charge transfer between, the atoms using Bader's method [28-30], which defines the boundary of an atom/ion by the zero-flux surfaces between that atoms/ions. This method is very helpful for understanding the nature of chemical bonding and charge transfer in solids [28-31]. This method has been incorporated into the *ab initio* code VASP and applied successfully for various materials [31-33].

IIc. Computational settings: VASP (Vienna *ab initio* Simulation Program) [34,35] was employed for all calculations. Density functional theory (DFT) within the Projector Augmented-Wave (PAW) method and the Generalized Gradient Approximation (GGA) [36,37] as formulated by Perdew, Burke and Ernzerhof (PBE) [38] was used. Spin-polarization was included for systems containing unpaired electrons as it was shown to be important earlier [39].

For all calculations, we employed E_{cut} = 550 eV for the valence electrons and E_{cut} = 700 eV for the augmented waves. The present settings are significantly higher than the corresponding default energy values of the potentials (E_{NMAX} = 400.00 eV for H, 322.069 eV for Si and 318.64 eV for B, respectively) in order to describe the strong B-Si, B-H bonding well. When using the same settings for all calculations, one expects the cancellation of systematic errors. The electronic wave functions were sampled on: (1) a 16×16×1 *k*-mesh (73 to 130 *K*-points depending on symmetry) for systems with a conventional lattice in-plane (Figure 1b), and (2) a 8×8×1 *k*-mesh (34 *K*-points) for systems with a $2a_1 \times 2a_1$ supercell (Figure 1d) in the Brillouin zone (BZ) of the Si(100) 2×1 surface using the Monkhorst and Pack method [40]. Tests of the *k*-meshes and cut-off energies show a good energy convergence (~1 meV/atom).

III. Results of the simulations and discussion

We will first address the calculated results for elemental molecules and solids. The calculations for an isolated H_2 molecule give a H-H bond length of 0.748 Å, which is just slightly larger than the experimental value (0.7414 Å) [41]. The calculations also show that an isolated BH_3 molecule has a planar structure with a B-H bond length of 0.965 Å, which is slightly larger than the corresponding experimental value (0.924 Å) [42]. Furthermore, our structural optimization of the diamond-type Si provides a lattice parameter of 5.494 Å, which is close to, but slightly larger than also the experimental value (5.431 Å) [27]. Such slight overestimations of the bond lengths/lattice parameters are not unusual for the density functional theory within the generalized gradient approximation [43].

We will start with the H-passivated Si(001) 2×1 surfaces. Figure 1a shows the schematic structure of the optimized H-passivated Si(100) 2×1 surface. Each Si is connected to two Si (d_{Si_Si} = 2.41 Å), one surface Si (d_{Si_Si} = 2.48 Å), and one H (d_{Si_H} = 1.49 Å). In this way the surface Si is also in a tetragonal coordination. The calculated Si-H bond length (1.49 Å) agrees well with the experimental value (d_{Si_H} = 1.49 Å) [19]. The Bader charge analysis shows the charge model for the surface atoms/ions: (-)$(Si1)^{+0.57}H^{-0.60}$. This charge transfer from Si to H is in accordance with the Pauling electronegativity difference between Si (1.9) and H (2.2).

To obtain detailed information about the deposited BH_n radicals at the Si(001) surface, we performed calculations for several types of configurations: a) direct deposition to form (-)Si-BH_n, b) exchanged Si and B to form (-)B-SiH_n, and c) BH_n at the surface with the formation of (-)BH_n. The calculated results are listed in Table I. Next we elaborate on these results.

Table I. Calculated results (formation energies, chemical bond lengths, and charges at the surface atoms) for BH_n (-Si-BH_n), exchange of the surface Si with the B (-B-SiH_n), and B at the surface. The results for the passivated Si(001) 2×1:H are included for comparison. The position of the defect states E_{defect} is set relative to the Fermi level (Fermi level is set at zero eV).

Cluster	ΔE (eV/BHn)	CNN(B)	*d*(Si-B)	*d*(B-H)	Charges (e)	E_{defect}*(eV)*
H	-	-	-	Si-H: 1..49	$-Si^{+0.62}H^{-0.61}$	1.41
BH_n radicals on surface Si, (-)Si-BH_n						
B	+4.228	1	2.04	-	$-Si^{+0.24}-B^{-0.36}$	+1.2
BH	+1.248	2	1.88	1.17	$-Si^{+0.64}-B^{-0.02}(H^{-0.62})$	+0.7
BH_2	-0.282	3	1.99	1.19	$-Si^{+0.46}-B^{+0.74}(H^{-0.60})_2$	
BH_3	-0.348	4	2.25	1.20	$-Si^{+0.12}-B^{+1.46}(^{-0.60})_3$	+0.2
Exchange between the surface Si and B in BH_n radicals on the Si surface, (-)B-SiH_n						
B-SiH	+1.383	3	1.97,2.04,2.05	-	$-B^{--1.37}-Si^{+1.06}(H^{-0.62})$	BH_ex
B-SiH_2	-0.295	3	2.01,2.04(x2)	-	$-B^{--1.37}-Si^{+1.80}(H^{-0.62})_2$	+1.0
B-SiH_3	-0.115	4	2.02, 2.15 2.13(x2)	-	$-B^{--1.07}-Si^{+2.32}(H^{-0.64})_3$	
BH_n radicals in the surface, (-)BH_n						
B	+1.778	3	2.07(×2), 2.14	-	$-B^{-1.08}$	0.89
BH	+0.895	4	2.13(×2), 2.15	1.20	$-B^{-0.01}(H^{-0.57})$	-
BH_2	+0.040	4	2.10, 2.13	1.20,1.38*	$-B^{+0.18}(H^{-0.60}H^{-0.55})$	+1.35
BH_3	-0.147	4	2.04	1.19, 1.20, 1.40$	$-B^{+0.89}(H^{-0.61})_2H^{-0.55}$	+0.88

*This H is connected to the B and one Si with Si-H 1.63 Å. $This H is also connected to another Si with Si-H bond length of 1.58 Å.

IIIa. Dilute BH_n (n=0 to 3) on Si(100) 2×1:H surfaces: Total energy calculations show that an isolated B on a Si(001) 2×1:H surface has a high positive formation energy (see Equations 2 and 3). This indicates that it is unfavorable to form naked B on the Si surfaces directly. H-passivation on the isolated B reduces the formation energy. However, as shown in Table I, the deposition of BH_2 and BH_3 radicals on the Si surfaces are favorable Deposition of isolated BH_n clusters on Si(001) 2×1:H surfaces also causes local structural relaxations (Figures 2a and 2c). The electronic structures of the two relatively stable configurations are shown in Figure 2b.

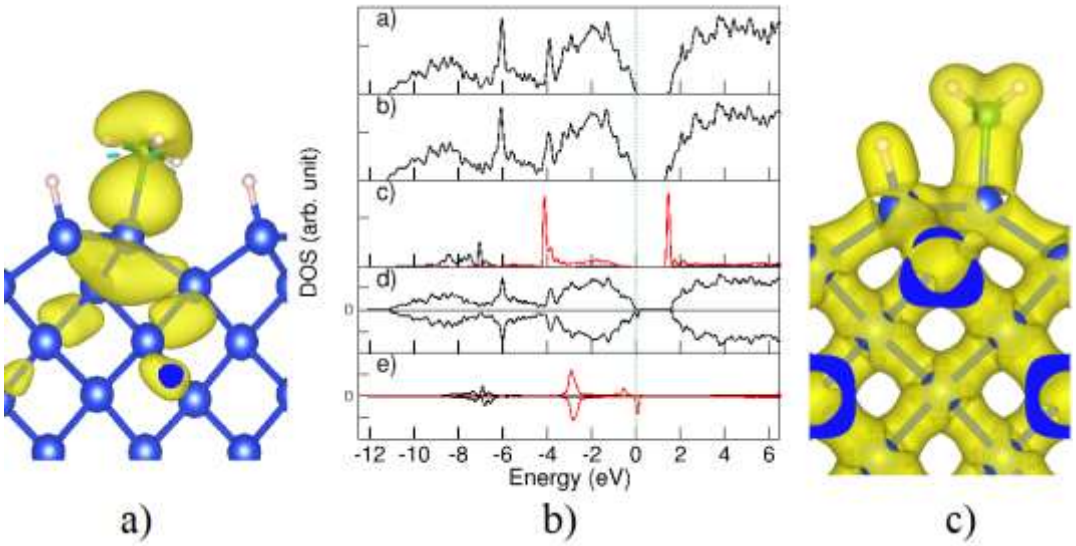

Figure 2. **(a)** Spin density iso-surface for one BH_3 on a Si(100) surface, **(b)** total and partial density of states (DOS) for the selected systems: (b_a) total DOS for the Si(001) 2×1:H surface; (b_b) total DOS for the surface with a BH_2 radical; (b_c) partial DOS for the B in the radical; (b_d) total DOS for the surface with a BH_3 radical; (b_e) partial DOS for the d B in the radical, and **(c)** electron density iso-surface for one BH_2 radical on the Si(100) surface. In Figures 1b_c and 1b_e, the black curves represent the partial DOS for the B-2s characters, and the red curves represent the B-2p states.

The total DOS is shown in Figure 2b_a (the top row) for the H-passivated Si(001)2×1 surface. Clearly it is composed of two well-separated parts. The valence band ranges from about -11.0 eV to the Fermi level (at zero eV). The conduction band starts at about 1.2 eV above the Fermi level. The bands in the lower part of the conduction band (CB) are not easily characterized. Some of them are rather dispersed, dominating the bottom of the CB. These states originate from the Si bulk. Meanwhile there are several almost non-dispersed bands positioned at about 0.3 eV above the bottom of the CB. These localized states come from the surface Si-H atoms/ions. Both the VB top and the CB bottom are at Γ. Therefore this slab is a direct gap semiconductor which differs from bulk Si. The calculations also show that this surface is spin-degenerated.

As shown in Figure 2b_b and 2b_d, the frames of the tDOS (total density of states) curves of the systems with one BH_n (n=2,3) deposition are analogous to that of the pure Si(001) 2×1:H surface. A detailed analysis shows the influence of the deposited BH_n radicals. The role of the BH_n (n=2 and n=3) varies in their electronic properties. For BH_2, the B-2s states exist in the energy range between -9.0 to -6.5 eV due to the strong interaction with the surface Si, while the B-2p states form two sharp peaks: one sharp peak occurs at about -4.2 eV, and another at the bottom of the conduction band (Figure 2b_c). These sharp B-2p peaks originate from the strong covalence between B and H (B 2p/H 1s). The unoccupied B-2p/H-1s states should be regarded as a defect state below the conduction band. The electronic structure calculations show that BH_3 deposited on the surface is spin-polarized with the spin at the BH_3 cluster (Figure 2c_d). In the structure, the B-2p/H-1s states form peaks at about -3.0 eV, one peak at about 0.2 eV below the Fermi level for the spin-up (majority) electrons, and another peak at about 0.2 eV above the Si:H VB for the spin-down (minority) electrons. The latter is unoccupied (Figure 2b_e). Therefore, the deposition of the BH_3 radical on the Si(001) 2×1:H surface produces a shallow defect state (i.e. holes). One

expects a strong impact of these defect states on the electronic and related optical and electrical properties of the system.

IIIb. Exchanging deposited B for the related surface Si: It is also of interest to study the possibility of doping B into the Si surfaces, by e.g. exchanging the B and its nearby Si to form (–B)-SiH_n configurations. The optimized structures, as well as the formation energies are shown in Figure 3 together with their electronic structure.

The structural optimizations show that there is structural reconstruction for the (–)B-SiH deposition. The surface B has three Si neighbors with bond lengths of 2.04 and 2.05 Å (Si from the subsurface surface layer) and of 1.97 Å to the Si on top. Meanwhile the Si on top of the surface B has three neighbors: one surface Si (Si-Si: 2.37 Å), one B (B-Si 1.97 Å) and one H (Si-H: 1.50 Å). The optimizations also show this kind of configuration is quite unstable with formation energy of about 1.383 eV, which is higher than that of the BH deposition (1.248 eV). Figure 3b shows the optimized structure of the (–)B-SiH_2 configuration of high stability (Table I). The surface B has three Si neighbors: two from the subsurface with a bond length of 2.04(×2) Å, and another deposited SiH_2 with a Si-B bond length of 2.01 Å. The original surface bridging B-Si is broken. Meanwhile, the deposited Si has four neighbors: two H (Si-H: 1.49 Å), the surface B (B-Si: 2.01 Å), and one surface Si (Si-Si: 2.42 Å). This means the deposited Si is connected to another surface Si to form a bridging Si-Si pair instead of the original B-Si pair. In this way the B is tri-coordinated and the deposited Si is 4-fold coordinated. The calculated formation energy is -0.295 eV, which is about 0.013 eV lower than that of the BH_2 deposition on Si (Table I).

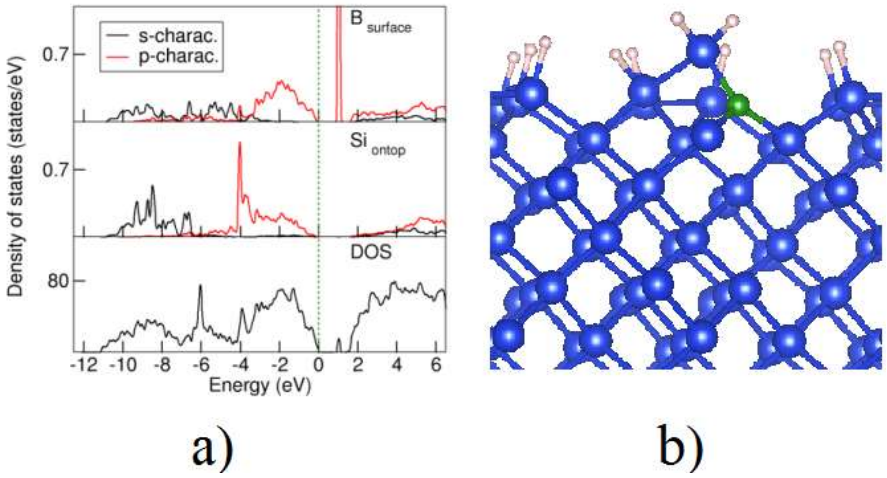

Figure 3. Total and partial DOS of the highly stable (-)B-SiH_2 system (a); and the related schematic structure (b).

For (-)$BSiH_3$, the surface B plays the role of the original Si with four Si neighbors: two from the subsurface (B-Si: 2.13 Å(×2)), one from the surface (B-Si: 2.15 Å) and one Si on top (B-Si: 2.02 Å). Meanwhile, the deposited Si also has four neighbors: three H (Si-H: 1.49 Å (×3)) and one surface B (B-Si: 2.02 Å). The total energy calculations provide the formation energy of -0.115 eV with respect to the surface and BH_3 cluster (Equations 2 and 3).

Figure 3a shows the total DOS and partial DOS of the important atoms/ions. Clearly the Si in the attached SiH_2 radical contributes a localized peak at 4.0 eV below the Fermi level. There are some dispersive states over the valence band due to the Si-Si bonding. Meanwhile, the surface B ion/atom has two parts: one part is dispersive over the upper side of the valence band and the lower part of conduction band, with a sharp peak (or isolated defect state) at about 1.0 eV above the Fermi level. Such a defect state should have notable effects on the electronic/electrical as well as optical properties of the system. It should also be noted that the B atoms/ions at the surface are negatively charged as summarized in Table I, which describes the major characteristics of the configurations.

The present simulations show local structural relaxation in all cases. The surface Si with a BH_n radical on top moves slightly (~0.1 to 0.2 Å) inwards. All the terminal H ions are negatively charged by about 0.6 e, with the H near Si being slightly more negatively charged than that near B (Table 1). This agrees with the high Pauling electronegativity (2.20) for hydrogen compared to 1.90 for silicon and 2.04 for boron. Structural analysis showed that more H atoms/ions on B, the Si-B bond lengths and the B-H lengths become longer. Simultaneously, the electron loss at the Si becomes smaller while the B becomes positively charged and the lost electrons are transferred to the terminal H ions. The calculations also show that the Si-B for the BH deposition has a length of 1.88 Å and Si loses 0.64 electrons (Table 1). When B becomes a surface ion/atom, it receives electrons from the Si neighbors and is negatively charged and a dangling B on top of a Si has a rather long Si-B distance. Charge analysis shows that B is negatively charged (Table 1).

Overall, the current calculations show that for n=1 and 3, the formation energies of the (-)B-SiH_n are less-favorable than the corresponding compositions with –Si-BH_n. Therefore this type of B-Si exchange is rather unlikely. However, for n=2, the configuration with the tri-coordinated B and 4 fold-coordinated Si in the (-)B-SiH_2 is more stable than that in the corresponding (-)Si-BH_2. That means B-Si exchanges may occur at the surface, especially at high temperature. The corresponding defect state in the forbidden gap will have an impact on the electronic and optical properties of the system. Furthermore, the surface B might move into the deep surface of the system.

The modelling of the BH_n depositions and related Si-B exchanges at the surface now allows us to evaluate the possibilities of BH_n radicals at the surface with the results in Table I.

Figure 4 shows the optimized structure of the systems with surface BH_n. The calculations show that the surface B has three Si neighbors (Figure 5a) with B-Si bond lengths of 2.07 Å (×2) and 2.14 Å. For the configuration in Figure 5b, the surface B has four neighbors: one H (B-H: 1.20 Å) and three Si (B-Si: 2.13 Å (×2) and 2.15 Å). Structural reconstruction occurs for the case in Figure 5c, where the surface B also has four neighbors: 2H (B-H: 1.20 Å and 1.38 Å) and 2 Si (B-Si: 2.10 Å and 2.13 Å). The H with a long B-H bond is also connected to one Si with a Si-H bond length of 1.38 Å. Similarly, in the case shown in Figure 5d, the B is coordinated four-fold with three H and one Si (Table I).

Note that the presented systems can be regarded as deposition of BH_n clusters on the Si(001) 2×1:H system with one surface Si missing. To estimate the formation energies for the systems containing a surface BH_n, Equations 2 and 3 are applied. The energy of the pure surface system is obtained by extracting the total valence electron energy of one bulk Si from the energy of pure $Si_{80}H_{16}$. As shown in Figure 4 and Table I, the formation energy decreases with the addition of H on B. The formation energies are positive for the B and BH clusters, while remaining only slightly positive for n=2 and turning negative for n=3. Considering their importance on devices, it is of importance to address the electronic properties of the systems as well. The obtained electronic structures are included in the supplementary materials, while the main characteristics are summarized in Table I.

As shown in Table I, the electronic structure calculations show that the stable (-)BH_3 configuration has a defect state of about 0.9 eV above the top of the valence band. Furthermore, the slightly metastable (-)BH_2 configuration has a defect state dominated by B-2p at the bottom of the conduction band. It is expected that such defect states have an impact on the electronic properties of the prepared system with depositions.

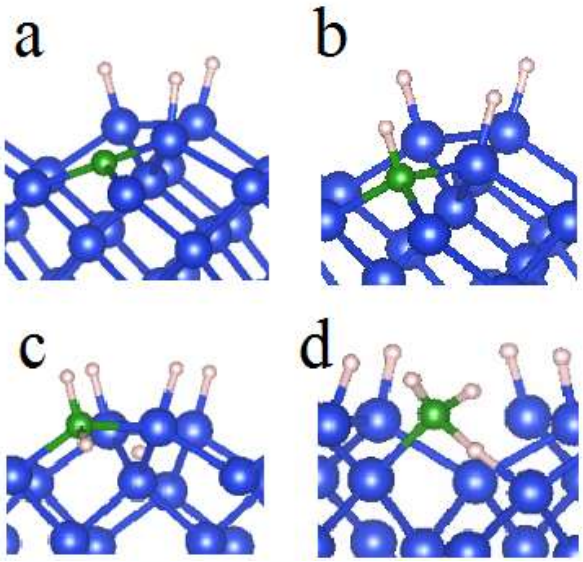

Figure 4. Schematic structure of the systems containing surface B (a, BH (b, BH2 (c and BH3 (d, at the Si(001) 2×1:H surface, respectively.

The simulations above provide information for dilute deposited BH_n on/at the Si(001) surface. To gain insight into the first step of the deposition process, information about a higher BH_n concentration is required. Therefore we also performed simulations for two BHn radicals deposited simultaneously at the surface. The results are shown in Table II.

IIId. Two BH_n radicals on the Si(100) 2×1:H surface: When two naked B atoms are deposited on the Si(001) 2×1:surface, strong structural reconstructions occur. For the B on the two bridging surface Si atoms (Table II), the two B atoms/ions form a bridge when the Si bridge is broken. The bridging B-B bond has a length of 1.49 Å, which is notably shorter than the bonds in the pure elemental boron solid (between 1.64 and 1.90 Å) and the Si-B bond (1.88 Å), being close to that of a BH cluster deposited on the Si surface (Table I). In the case of B deposited on two separated surface Si atoms, structural optimizations show local reconstruction. The formation energies range from about 4.2 eV per B to about 2.5 eV per B for the two nearby B atoms (Figure 6a), and reach about 2.2 eV per B for the two separated B atoms (Figure 6b). However, overall the

formation energies for the naked B on the surface are still positive with large values (>2.0 eV per B). One BH on top of bridging Si atoms also forms a bridging B-B pair. Therefore, each B is threefold coordinated to one Si, one B and one H. As compared with isolated BH deposition on the Si surface with a formation energy of 1.25 eV per BH (Table I), the formation energy of this configuration is much smaller (0.876 eV per BH) for two BH molecules on two separated Si atoms, where the B is bridging between two surface Si atoms while the original Si-Si bridge is broken. The calculated formation energy is about 1.04 eV per BH, which is in between that of the isolated BH deposition (Table I) and that of the configuration with a B-B bridge.

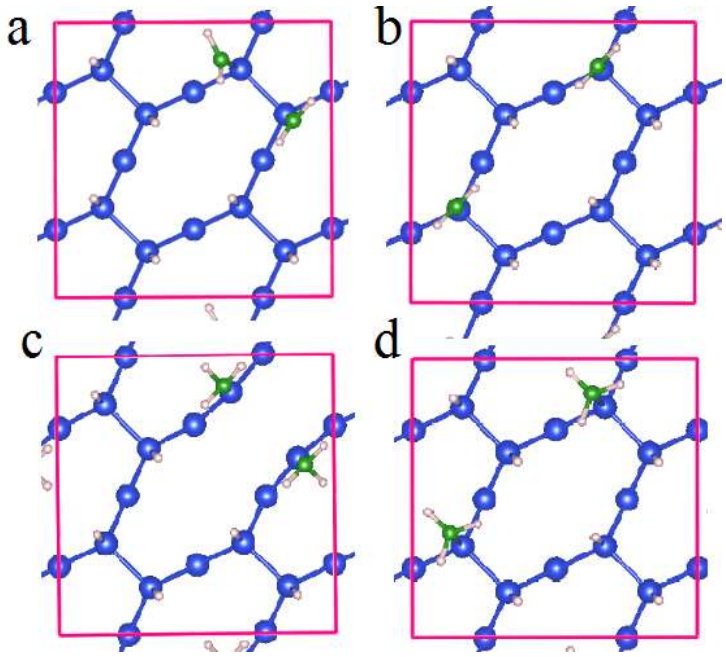

Figure 5. Schematic structures and formation energies of two BH_2 clusters: (a) on top of two bridging Si atoms (close to each other), (b) on two separated surface Si atoms, (c) on two BH_3 clusters on two bridging Si atoms, and (d) on two separated Si atoms. It is noted the calculations showed that all the configurations are stable with respect to the H-passivated surface and BH_3 molecules (Equations 2 and 3). The most stable one is two BH_3 clusters on two bridging Si atoms/ions. Structure optimizations showed that Si-Si bond between the bridging Si atoms/ions is broken due to the BH_3 deposition (Figure 5c).

As shown in Figure 5, all the configurations for the two BH_2 and BH_3 clusters on the Si(001) 2×1:H surfaces are stable with respect to the Si:H surface and BH_3 molecules, according to Equations 2 and 3. In fact the formation energies of the two BH_2 clusters on the Si(001) surface are quite close to that of one BH_2 deposition. This agrees with similar local structures as shown in Figure 5a and 5b. This is also true for the two BH_3 clusters on two separated Si atoms (Figure 5d). Meanwhile, structural optimization shows that the deposition of two BH_3 clusters on two bridging Si atoms is reconstructed (Figure 5c). The Si-Si bridge is broken and each of the Si atoms/ions now has only three neighbors (two from the subsurface and one B). The B has one Si neighbor and three H atoms on top. This structure is very stable with a formation energy of about -0.79 eV per BH_3, which is notably lower than BH_n ($n\neq3$) (Tables I and II).

Table II. Calculated results (formation energies, coordination number of nearest neighbors for boron (CNN(B)), chemical bond lengths, and charges at the surface atoms) for two -BH_n (n=0 to 3) clusters at the surface. The position of the defect states E_{defect} is set above the Fermi level.

Cluster	ΔE (eV/BH_n)	CNN(B)	d(Si-B)	d(B-H)	Charges (e)	E_{defect}(eV)
2B_cls	+2.450	2	1.88 B-B: 1.49	-	-	0.91
2B_sep	+2.199	3	1.93, 2.07(×2)	-	$-B^{-1.35}$	1.10
2BH_cls	+0.876	3	2.03 B-B: 1.73	1.19	$-B^{+0.23}H^{-0.61}$	0.51
2BH_sep	+1.039	3	1.97, 2.00	1.19	$-B^{-0.37}H^{-0.60}$	0.52
$2BH_2$_cls	-0.276	3	2.00	1.19(×2)	$-B^{+0.70}(H^{-0.60})_2$	1.41
$2BH_2$_sep	-0.282	2	1.99	1.19(×2)	$-B^{+0.72}(H^{-0.60})_2$	1.46
$2BH_3$_cls	-0.785	4	1.93	1.19(×2),1.37*	$-B^{+1.0}(H^{-0.58}H)_2H^{-0.54}$	1.41
$2BH_3$_sep	-0.325	4	2.30	1.20(×3)	$-B^{+1.48}(H^{-0.59})_3$	+0.10

*This H is also connected to another Si with a longer Si-H distance of 1.71 Å.

Table II also includes the corresponding electronic properties. Clearly, for the two BH_2 clusters deposited on the Si surface, the electronic structure is quite similar to that of an isolated case (Table I). It is understandable since the local structure and chemical bonding in the denser case are quite similar to that of the isolated case. For the BH_3 cases, when the two clusters are

separated, the electronic structure is also similar to that of the single molecule case. There is an unoccupied defect state at about 0.2 eV above the Fermi level. Moreover, when the two clusters are set at two bridging Si-Si pair, structural reconstruction not only strongly stabilizes the system, but also changes the electronic nature. There is an unoccupied state just below the bottom of the conduction band, which is significantly different from those in the case of the two BH_3 clusters positioned on two separated Si atom/ions. This stabilization of BH_3 clustering may play an important role in the Si/B structures in the PureB process as well as in the electronic properties of the products.

In short, the calculations show similarity between the structures and electronic properties for the two BH_n clusters as compared with all cases except for n=3. The high stability of the reconstructed 2-BH_3 clustering indicates possibilities for further deposition, deserving further investigation.

IIIe. Discussion: PureB at the *initial* stage: First we summarize the calculated energetics of B_mH_n (m=1,2; n=0 to 3) on the Si(001) 2×1:H surface. As presented above, the dependences of the formation energies of the BH_n (n=0 to 3) clusters deposited on the Si sites are complex for low coverage, as shown in Figure 6.

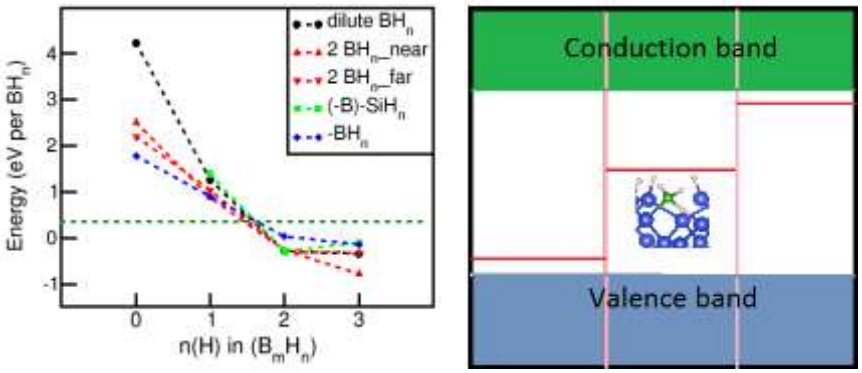

a) b)

Figure 6. Dependences of the formation energies on the H concentration of the BH_n radicals on the Si surfaces with different concentrations (a), and the schematic electronic structure of the defect states in the forbidden energy gap of the deposited Si(001) 2×1:H surface (b).

Overall, the number n (of H atoms) in the BH_n clusters plays a dominant role. Depositions of B and BH clusters on the surface cost energy and are unstable with respect to the H-passivated Si(001) 2×1 surface and BH_3 molecules which are produced in the B_2H_6 decompositions in the PureB deposition process [1-7]. Meanwhile the negative values of the formation energies for the BH_n (n= 2,3) clusters on the Si surface imply possible depositions. Furthermore, the configuration of –B-SiH_2 shows exceptionally high stability. This indicates the possibility of surface B formation. This is a mechanism for B to incorporate into Si to form strong Si-B bonding, i.e. to form a B-Si interface at the *initial* stage. Considering the high activation energy of B diffusion in Si (3.25 to 3.80 eV) [45-47], B can only diffuse into Si to from a Si/B mixing layer (electrically 'dead layer'), and/or to form a P-type region due to B-doping at high temperature, typically about 600° to 700°, as shown in the experimental observation [1-6]. Overall, the calculations also show that BH_n clustering may further increase the stability of the depositions.

From the above energetics, we can propose a series of deposition reactions. As shown experimentally, one diborane molecule decomposes into two boron tri-hydride molecules, as shown in Equation 1. At elevated temperature, the H ions/atoms on the surface are desorbed and leave dangling Si bonds. Then the BH_3 molecules deposit on the surface Si dangling bonds to form –Si-BH_3 clusters of high stability.

The configuration (-)Si-BH_3 has the lowest formation energy (Table I and Figure 6). Moreover, the configuration –Si-BH_2 is also quite stable. Therefore, we assume the reaction: -Si-BH_3 ↔ -Si-

BH_2 + ½ H_2 + ΔH_1. Note that in this reaction, there are H_2 molecules produced. At elevated temperature, e.g. T = 700 K, the contribution of entropy of half a H_2 molecule is $(3k_BT)/2$~0.088 eV (here 2 is di-atomic), which is larger than the formation energy difference between the two configurations -(-0.348 –(-0.282)) = 0.066 eV. Then we obtain the free energy difference: ΔG (= $\Delta H_1 - \Delta S\ T$) = -0.022 eV. This means that at about 700 K, many -Si-BH_3 configurations may transfer to the –Si-BH_2 structure. Therefore, we investigated the energy barrier for the decomposition of two nearby (-Si)BH_3 to form two (-Si)BH_2 and one H_2 molecule using the step by step approach which is similar to the well-known Nudged Elastic Band method [47,48]. The calculation details and results are as follows.

As shown in Figure 5c, the two BH_3 molecules on the Si surface have mirror symmetry. The Si-Si bridging bond is broken. We draw two nearby H atoms, each from the opposite BH_3 molecule gradually closer to each other by fixing their in-plane coordinates and their z-component of coordinates is set free. The calculated energy difference with respect to that of the configuration in Figure 5c (two BH_3 molecules on two nearby Si atoms) depends on the H-H distance, As shown in the new figure (Figure 7).

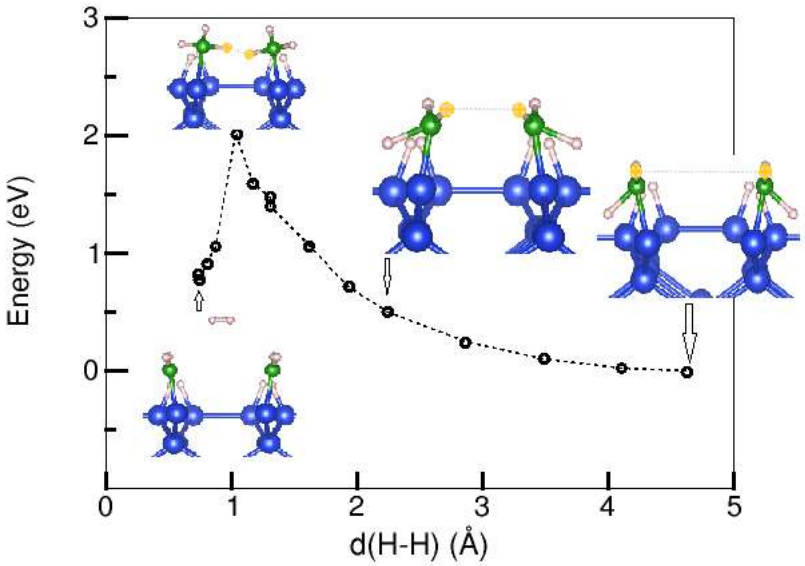

Figure 7. The calculated energy difference with respect to the energy of the configuration in Figure 5c on the H-H interatomic distance. Several schematic configurations are inserted, in which the large spheres represent for Si, middle green spheres for B and small white spheres for H. The dotted line linked small spheres with light-orange color represent the two H ions/atoms in reaction to form a H_2 molecule (a linked white sphere pair) as shown in the last inserted at the left and lower position of the figure .

Clearly with the shortened H-H distance, the related BH_3 molecules rotate and the central B atoms also move close to each other. Correspondingly, the energy of the system rises and reaches a maximum at *d*(H-H) of about 1.0 Å.

Then, with the weakening of the H-B bond, the B atoms with their two remaining H ions return to the original positions and the energy goes down. The energy reaches its minimum when the d(H-H) is being about 0.74 Å, the interatomic distance of a lone H2 molecule from our calculations (Figure 7). Next, the H_2 molecule moves away. The energy barrier in this calculation is about 2.1 eV with respect to that of the original configuration (Figure 5c).

The present calculations also produced another rather stable configuration with energy close to that of the original configuration (just about 0.1 eV higher in energy). This structure has H bonded to the two B atoms and another H bonding to one of the Si, as shown in the attached.

This work indicates that simple NEB method can provide useful information about the reaction paths and related energy barriers. Knowledge of such barriers is very helpful for investigating the reaction paths and energetics of the reactions proposed in our manuscript. However, the great

complexity and number of reaction pathways has made it impossible to generate a more complete picture for these reactions.

The–Si-B_2 thus formed may further transfer to the –B-SiH_2 configuration to form surface B which may diffuse deep into the slab at elevated temperature. Another option is the formation of BH_n clustering at the *initial* stage. This occurs only if a high concentration of dangling Si exists. From the above discussion, we can conclude the following possible stable configurations: (-)Si-BH_3, (-)Si-BH_2, and (-)B-SiH_2. These configurations have different contributions to the electronic properties of deposited systems. The direct deposition of (-)Si-BH_3 produces an electronic hole on the surface. On the other hand, the (-)B-SiH_2 and (-)BH_3 configurations create unoccupied B-2p states at about 1.0 eV above the valence band. The B-2p states of the relatively stable (-)Si-BH_2, and clustered Si-BH_3 are just below the conduction bands as shown in Tables I and II. These defect states from the stable configurations at the *initial* stage, therefore, have a strong impact on the electrical and optical properties.

V. Conclusions

First-principles structural optimization and total energy calculations have been performed for BH_n cluster depositions on Si(001) 2×1:H surfaces in a systematic way. The calculations showed strong chemical bonding between the deposited borane radicals and the silicon surface. The order of stability for BH_n deposition at T = 0 K is: BH_3 > BH_2 >>BH >>B. The calculations show that (-)Si-BH_2 may convert to (-)B-SiH_2. This indicates incorporation of B in Si surfaces. Thermodynamic analysis also shows a strong temperature dependence of the chemical reactions

with formation of (-)Si-BH_2 or (-)B-SiH_2 becoming more favorable because of the entropy contribution of H_2 gas.

Electronic structure calculations show the impact of the BH_n deposition on the electronic properties, e.g. local spin-polarization and electronic holes due to the BH_3 deposition on the surface. This influences the charge carriers and electrical transport properties.

From the present study, it is expected that B-Si interfaces can be regulated to be sharp because of the rather low temperature in the PureB process. As shown in earlier experiments [5-7], such sharp/atomic layer-thick B-Si junction layers are expected to have unusual physical properties. Furthermore, the incorporated B can diffuse into Si to form p-type Si with B doping and/or to form a thick Si/B region, depending on the preparation conditions (temperature, time, *etc*.). This routine can explain the relationship between the obtained B-Si junctions and the PureB conditions, e.g. formation of a Si/B 'dead layer' at high temperature [1-7]. The present study also indicates that higher BH_n coverage increases the stability of the system and produces more defect states in the energy gap, which leads to formation of an amorphous B layer. This agrees with the experimental results that the final PureB products contain a thin layer of B on the Si surfaces.

References

1. F. Sarubbi, L. K. Nanver and L. M. Scholters, IEEE Trans. Electron Devices 57, 1260 (2010).

2. L. Shi, F. Sarubbi, L. K. Naver, U. Kroth, A. Gottwald and S. Nihtianov, Procedia Eng. 5, 633 (10210).

3. V. Mohammadi, W. B. de Boer and L. K. Naver, Appl. Phys. Lett. 101, 111906 (2012).

4. V. Mohammadi, W. B. de Boer and L. K. Naver, J. Appl. Phys. 112, 113501 (2012).

5. V. Mohammadi, W. B. de Boer, T. L. M. Scholtes and L. K. Naver, ECS Transactions 45, 57(2013).

6. F. Sarrubbi, L. K. Nanver and T. L. Scholters, ECS Transactions 3, 35(2006).

7. V Mohammadi, PR Rao, RWE van de Kruijs, S Nihtianov, Device Research Conference (DRC), 73rd Annual, 73-74 (2015)

8. S. H. Bauer, J. Am. Chem. Soc. 59, 1096 (1937).

9. R. P. Clarke and R. N. Pease, J. Am. Chem. Soc.73, 2132 (1951).

10. J. K. Bragg, L. V. McCarty, and F. J. Norton, J. Am. Chem. Soc. 73, 2134 (1951).

11. S. H. Bauer, Energetics of the Boranes. V. J. Am. Chem. Soc. 80, 294 (1958).

12. T. P. Fehlner, J. Am. Chem. Soc. 87, 4200 (1965).

13. S. Komatsu, M. Kasamatsu, K Yamada and Y. Moriyoshi, J. Appl. Phys. 71, 5654 (1992).

14. K. Sato, N. Kanda, T. Ogata and Y. Kumashiro, Chem. Phys. Lett. 325, 453 (2000).

15. K. Sato and Y. Kubota, Applied Physics Express, 4 , nr. 5 (2011).

16. H. Habuka, S. Akiyama, T. Otsuka, and W. F. Qu, J. Crystal Growth, 209, 807 (2000).

17. J. B. Hannon, H. Hibino, N. C. Bartelt, B. S. Swartzentruber, T. Ogino and G. L. Kellogg, Nature 405, 552(2000).

18. A.Ramstad, G. Brocks and P. J. Kelly, Phys. Rev. B 51, 14504(1995).

19. K. A. Perrine and A. V. Teplyakov, Chem. Soc. Rev. 39, 3256(2010).

20. M. Hakala, M. J. Puska, and R. M. Nieminen, Phys. Rev. B 61, 8155(2000).

21. X. D. Pi, X. B. Chen and D. R. Yang, J. Phys. Chem. C 115, 9838 (2011).

22. V. G. Zavodinsky, E. N. Chukurov, and I. A. Kuyanov, Surf. Rev. Lett. 16, 167(2009).

23. K. Boukari, P. Sonnet and E. Duverger, Chemphyschem. 13, 3945 (2012).

24. F. Shayeganfar and A. Rochefort, J. Phys. Chem. C 119, 15742 (2015).

25. A. Rose, Nuclear Instruments and Methods 52, 166 (1967).

26. S. W. Hu, Y. Wang, Y; and X. Y. Wang; J. Phys. Chem. A 107, 1635 (2003).

27. R. W. G. Wyckoff, *Crystal Structures*, John Wiley, New York (1963).

28. R. F. W. Bader and P. M. Beddal, Chem. Phys. Lett. 8, 29 (1971).

29. R. F. W. Bader, T. T. Nguyen and Y. Tal, Prog. Phys. 44, 893(1981).

30. R. F. W. Bader, J. Phys. Chem. A. 102, 7314 (1998).

31. G. Henkelman, A. Arnaldsson and H. Jónsson, Comput. Mater. Sci. 36, 254 (2006).

32. C.M. Fang, W.-F. Li, R.S. Koster, J. Klimeš, A. van Blaaderen, and M.A. van Huis, Phys. Chem. Chem. Phys., 17, 365 (2015).

33. C. M. Fang, A. van Blaaderen and M. A. van Huis, J. Phys. Chem. C 119, 14343 (2015).

34. G. Kresse and J. Hafner, Phys. Rev. B 49, 14251 (1994).

35. G. Kresse and J. Furthmüller, J. Comput. Mater. Sci. 6, 15 (1996).

36. P. E. Blöchl, Phys. Rev. B 50, 17953 (1994).

37. G. Kresse, and J. Joubert, Phys. Rev. B 59, 1758 (1999).

38. J. P. Perdew, K. Burke and M. Ernzerhof, Phys. Rev. Lett. 77, 3865(1996).

39. R. Wu and S. L. Lee, International Journal of Quantum Chemistry 79, 47 (2000).

40. H. J. Monkhorst and J. D. Pack, Phys. Rev. B 13, 5188 (1976).

41. K. P. Huber, G. Herzberg, *Molecular Spectra and Molecular Structure. IV. Constants of Diatomic Molecules*, Van Nostrand Reinhold Co. (1979).

42. R. Lide, CRC *Handbook of Chemistry and Physics*, 84th Edition. CRC Press. Boca Raton, Florida, (2003).

43. R. O. Jones, Rev. Modern Phys. 87, 897 (2015).

44. K. Momma and F. Izumi, J. Appl. Crystallogr., 44, 1272 (2011).P. M. Fahey, P. B. Griffin and J. D. Plummer, Rev. Modern Phys. 61, 289 (1989):

45. M. Mirabella, D. De Salvador, E. Napolitani, E. Bruno and F. Priolo, J. Applied Phys. 113, 031101 (2013).

46. W. Windl, M. M. Bunea, R. Stumpf, S. T Dunham and M. P. Masquelier, Phys. Rev. Lett. 83, 4345 (1999).

47 G. Henkelman and H. Jónsson, *J. Chem. Phys.* **113**, 9901 (2000).

48 G. Henkelman and H. Jónsson, *J. Chem. Phys.* **113**, 9978 (2000).